Temporal phase unwrapping: application to surface profiling of discontinuous objects

H. O. Saldner and J. M. Huntley

The recently proposed technique of temporal phase unwrapping has been used to analyze the phase maps from a projected-fringe phase-shifting surface profilometer. A sequence of maps is acquired while the fringe pitch is changed; the phase at each pixel is then unwrapped over time independently of the other pixels in the image to provide an absolute measure of surface height. The main advantage is that objects containing height discontinuities are profiled as easily as smooth ones. This contrasts with the conventional spatial phase-unwrapping approach for which the phase jump across a height discontinuity is indeterminate to an integral multiple of 2π. The error in height is shown to decrease inversely with the number of phase maps used. © 1997 Optical Society of America

Key words: Phase unwrapping, profilometry, shape measurement, projected fringes, grating methods.

1. Introduction

The use of projected fringes for the measurement of surface profile is a well-developed technique.[1–3] Parallel fringes are projected onto the object surface, either by a conventional imaging system or by coherent light interference patterns. If the projection and observation directions are different, the phase distribution of the measured fringe pattern includes information on the surface height profile of the object. The sensitivity can be improved by viewing through a line grating: the technique is then referred to as projection moiré.

An automated analysis of the fringe patterns is normally carried out either by the Fourier transform method or by phase stepping of the fringe patterns. Both produce wrapped phase maps (i.e., phase values lying in the range $-\pi$ to $+\pi$); the 2π phase jumps must then be removed by the process known as phase unwrapping to recover the surface shape. Phase unwrapping is normally carried out by comparing the phase at neighboring pixels and adding or subtracting multiples of 2π to bring the relative phase between the two pixels into the range $-\pi$ to $+\pi$. This causes problems when the technique is applied to real engineering objects, because such objects often contain sudden jumps in profile.[4] It can then become impossible to unwrap correctly across such real discontinuities, and large (multiples of 2π) phase errors can propagate across the image. The problem can be reduced in principle by measuring several phase maps at different sensitivities.[5–7] Only one unwrapped map will then be consistent with all the wrapped maps. White-light interferometry can also measure absolute surface heights,[8] but it is difficult to apply when the height variations exceed the range of a piezoelectric translator (PZT), typically a fraction of a millimeter.

In this paper we show how the temporal phase-unwrapping method described in Ref. 9 can be applied to the problem of profiling discontinuous objects. The basic idea is to vary the pitch of the fringes over time. A sequence of phase maps is recorded, forming a three-dimensional phase distribution. The phase at each pixel is then unwrapped along the time axis; because the unwrapping path does not cross object discontinuities, 2π phase errors do not propagate across the image as with conventional spatial unwrapping approaches. The method is simple and robust. In the case of coherent light projection systems, the technique also has the advantage that aberrations in the system are automatically canceled so that high-accuracy measurements can be made without the need for calibration with a flat reference surface.

H. Saldner is with the Division of Experimental Mechanics, Luleå University of Technology, Luleå S-97187, Sweden. J. Huntley is with the Department of Mechanical Engineering, Loughborough University of Technology, Loughborough LE11 3TU, UK.

Received 4 April 1996; revised manuscript received 7 October 1996.

0003-6935/97/132770-06$10.00/0

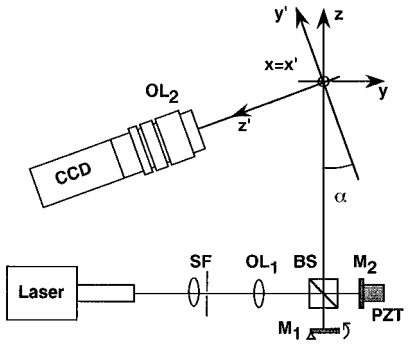

Fig. 1. Optical arrangement for shape measurement by projected fringes: SF, spatial filter; OL_1, objective lens (collimator); OL_2, objective lens (image formation); BS, beam splitter; M's, mirrors; PZT, piezoelectric translation stage; CCD, video camera.

2. Temporal Phase Unwrapping Applied to Surface Profiling

Here we show how temporal phase unwrapping can be used to extract surface profiles from phase measurements made by a fringe projection system of variable sensitivity. For simplicity, coherent collimated light projected fringes are considered here, but the same principle can be easily extended to other projection systems.

A coherent light system consists of two beams of light propagating almost colinearly. A Michelson interferometer (see Fig. 1) is one convenient means of achieving this.[1] The two beams will be denoted A and B; they are assumed to be collimated and to have equal amplitudes a_0. Mirror M_1 controls the angle of beam A. When the tth fringe pattern is recorded ($t = 0, 1, 2, \ldots, s$) the complex amplitudes of the beams in the (x, y, z) coordinate system of Fig. 1 can be written as

$$a_A(x, y, z, t) = a_0 \exp\{i[k_x(t)x + k_y(t)y + k_z z + \phi_A(x, y)]\}, \quad (1)$$

$$a_B(x, y, z) = a_0 \exp\{i[k_z z + \phi_B(x, y)]\}, \quad (2)$$

where $\mathbf{k} = (k_x, k_y, k_z)$ is the wave number of the light ($|\mathbf{k}| = 2\pi/\lambda$, where λ is the wavelength) and ϕ_A and ϕ_B represent, for example, the curvature of the wave front that is due to aberrations in the system or a small initial tilt relative to the z axis. Here $k_x(0)$ and $k_y(0)$ are defined to be zero. The change in k_z is zero to first order in k_x and k_y and can therefore be neglected for small tilts.

The beams intercept the object surface and the scattered light from both beams leaving a given point (x, y, z) on the object travels along the same optical path onto the image plane. The phase between the scattered light from the two beams can be measured (for example by using the phase-stepping method),[7] giving

$$\Phi(t) = \phi_B(x, y) - \phi_A(x, y) - k_x(t)x - k_y(t)y. \quad (3)$$

The phase change produced by tilting the mirror for the sth map is

$$\Phi(s) - \Phi(0) = -k_x(s)x - k_y(s)y. \quad (4)$$

In the coordinate system (x', y', z') of the object, where $z' = z'(x', y')$ is the surface profile to be measured, the change can be written as

$$\Phi(s) - \Phi(0) = -k_x(s)x' + k_y(s)(y' \sin\alpha + z' \cos\alpha), \quad (5)$$

where α is the projection angle measured relative to the reference plane $z' = 0$. If the phase surface $\Phi(s) - \Phi(0)$ can be unwrapped correctly, the plane $\Phi_P = -k_x(s)x' + k_y(s)y' \sin\alpha$ can be subtracted to give a phase map directly proportional [with a scaling factor $k_y(s)\cos\alpha$] to the height profile of interest. The effect of the optical system's aberrations is canceled out, and provided the values $k_x(s)$, $k_y(s)$, and α are known, no reference plane is therefore required for calibration purposes.

The unwrapped phase change $\Phi(s) - \Phi(0)$ will not in general lie within the range $(-\pi, +\pi)$ for all points in the image because there will normally be at least several fringes across the field of view. The temporal phase-unwrapping algorithm[9] can be applied here, provided a sequence of phase maps $\Phi(t)$ ($t = 1, 2, \ldots, s$) is acquired during the tilting procedure such that the time-varying phase at each pixel is measured at least twice per cycle. If $k_x(t) = 0$ and the object is known to be contained within the rectangular region $-Y < y' < Y$, $-Z < z' < Z$, then the change in k_y between any two phase measurements must satisfy the equation

$$k_y(t) - k_y(t-1) < \pi/(Y \sin\alpha + Z \cos\alpha). \quad (6)$$

Physically, this corresponds to the introduction of no more than one additional fringe across the field of view between two successive measurements and requires mirror M_1 to be tilted by a constant angle between each pair. The sequence of phase values at each pixel can then be unwrapped by adding or subtracting integral multiples of 2π to bring the phase change between any two phase values into the range $(-\pi, \pi)$. As noted in Ref. 9, this unwrapping procedure becomes particularly simple in the case of a phase-stepping analysis of the fringes. For example, in the four-frame technique,[7] incremental phase maps

$$\Delta\Phi(t) = \Phi(t) - \Phi(t-1) \quad (7)$$

can be calculated as

$$\Delta\Phi(t) = \tan^{-1}\left[\frac{\Delta I_{42}(t)\Delta I_{13}(t-1) - \Delta I_{13}(t)\Delta I_{42}(t-1)}{\Delta I_{13}(t)\Delta I_{13}(t-1) + \Delta I_{42}(t)\Delta I_{42}(t-1)}\right], \quad (8)$$

where

$$\Delta I_{ij}(t) = I_i(t) - I_j(t). \quad (9)$$

The sth phase map can then be calculated by simply summing the phase differences, with no further unwrapping required:

$$\Phi(s) - \Phi(0) = \sum_{t=1}^{s} \Delta\Phi(t). \tag{10}$$

3. Experimental

The temporal phase-unwrapping approach to surface profilometry was tested experimentally by using the apparatus shown in Fig. 1. The beam from an 80-mW frequency-doubled diode-pumped YAG laser ($\lambda = 532$ nm) was spatially filtered and then collimated by objective lens OL_1. The angle between the two beams was adjusted by tilting mirror M_1; it was possible to do this manually for the relatively small fields of view considered here, though the use of a PZT tilting stage would be desirable for larger objects. Phase steps of $\pi/2$ were introduced between successive TV frames by moving mirror M_2 on a PZT translation stage. Objective lens OL_2 was a Nikon 35-135 zoom lens. The focal length used during the experiments was approximately 100 mm, and the aperture ratio of $f/3.5$ gave a speckle diameter of 3.5 μm. This compares with an active pixel area of $5.8 \times 7.4\ \mu m^2$: it is important to have several speckles per pixel, otherwise speckle noise can become significant.

The images were acquired by using the electronic holography system at Luleå University of Technology, which was developed at the United Technologies Research Centre.[10] The system incorporates a pipeline processor that allows fringe patterns corresponding to the change in phase distribution to be displayed in real time. Sequences of typically 20–30 incremental phase-stepped images were saved on disk for each of the objects investigated. The images were then transferred to a Sun Sparcstation 5 computer for further analysis. Incremental phase maps were determined by Eq. (8) by using the FORTRAN function ATAN2 to calculate the required four-quadrant inverse tangents.

Figure 2 shows wrapped phase maps of the three objects under investigation. The first [Fig. 2(a)] was a test object consisting of three 4-mm-wide vertical grooves, on 6-mm centers, machined in a flat piece of plastic. The edges of the first and third grooves are visible on the left and right sides of the image. The depths of the three grooves were approximately 1, 2, and 4 mm. It is impossible to unwrap this phase map correctly by conventional spatial methods because the phase jumps at the groove edges are too large [they fall outside the range $(-\pi, \pi)$]. The relative depths of the grooves are therefore uncertain to integral multiples of 2π. The test object was illuminated along the grooves to avoid shadowing, i.e., from below in Fig. 2(a). Figure 2(b) is a wrapped phase map of an integrated circuit on Veroboard; again the height of the pins relative to the top surface cannot be determined from this single image. Figure 2(c) is a map of a molar tooth and two neighbors from a dental training mouth. There is no unwrapping path from one tooth to the next, so their relative heights cannot be determined by the conventional method. The integrated circuit and teeth were measured as found, without painting their surfaces. The camera was turned 90° in the last two experiments; thus they were illuminated from the right in Figs. 2(b) and 2(c). Angle α was set to 20° [Fig. 2(a) and 2(b)] and to 40° [Fig. 2(c)].

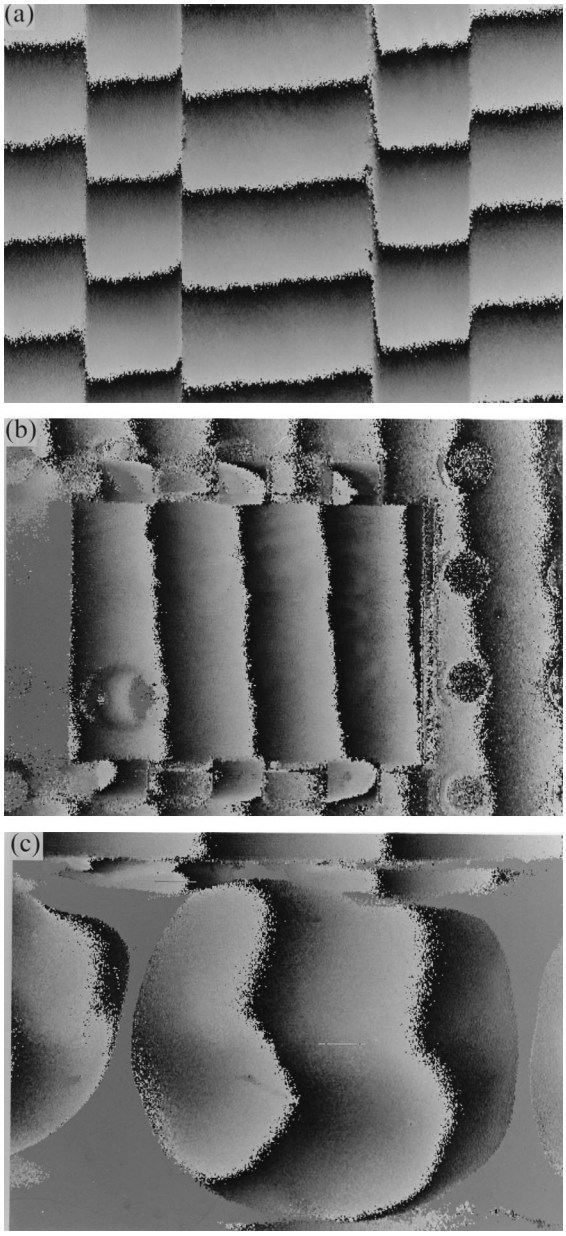

Fig. 2. Wrapped phase maps, showing shapes of discontinuous objects: (a) test plate containing vertical grooves of varying depths, (b) six-pin integrated circuit on circuit board, (c) two adjacent teeth from a replica of a human jaw. Black and white represent phases of $-\pi$ and $+\pi$, respectively.

When the incremental phase maps were calculated by Eq. (8), it was found that the phase change at the center of the measurement volume ($x' = y' = z' = 0$) was nonzero. This was because the rotation axis for mirror M_1 did not pass through the center of beam A

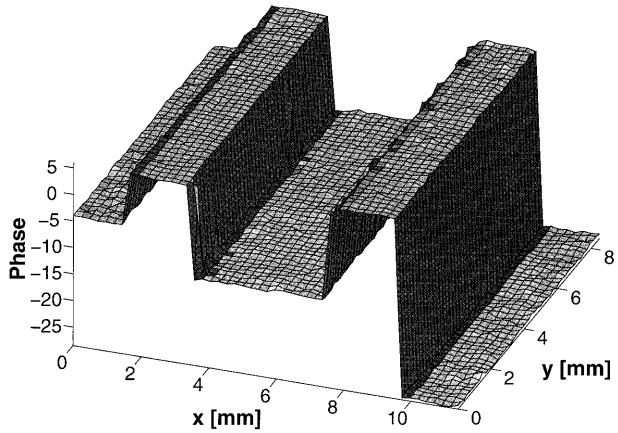

Fig. 3. Phase map from Fig. 2(a) unwrapped by the temporal phase-unwrapping algorithm, using 22 incremental maps.

so that the fringes moved in from one side of the field of view rather than equally from both sides. The phase at the center of each incremental phase map was therefore subtracted from all the phase values in the image, and 2π was added or subtracted as necessary to keep them all within the range $-\pi$ to π. This allowed a greater tilt to be made between two successive exposures.

Once the final phase change $\Phi(s) - \Phi(0)$ was calculated by Eq. (10), the values of $k_x(s)$ and $k_y(s)$ were obtained by least-squares fits along two perpendicular directions of a reference plane, which was arranged to be within the field of view. This was necessary to obtain the scaling factor relating phase to depth because the amount of tilt introduced was not known precisely; as noted above, the need for such a reference surface would have been avoided if the movement of M_1 could have been more precisely controlled.

4. Results and Discussion

Figure 3 shows the result of unwrapping the phase map of Fig. 2(a) through 22 intermediate images. The differences in height between the three grooves have been successfully detected. This has been achieved by direct implementation of the temporal phase-unwrapping algorithm [Eq. (10)] without data smoothing, windowing, or manual intervention; this would not have been possible with any of the existing spatial phase-unwrapping algorithms.

Calculated cross sections along row 256 [approximately halfway up Fig. 2(a)] are shown in Fig. 4 for different values of s, the number of incremental phase maps used during unwrapping. Figure 4(a) is the result of just a single map, whereas $s = 6$ and 22 for Figs. 4(b) and 4(c), respectively. Figure 4(c) is the cross section through the surface plot shown in Fig. 3. The reduction in noise that occurs as the experiment progresses is significant. Figure 4(a) is the result that would have been obtained with a conventional projected-grating method of very high grating spacing and therefore low sensitivity. Although the steps have been successfully detected, the signal-to-noise ratio is poor. Each incremental phase map looks broadly similar to Fig. 4(a). It is therefore intuitively appealing to regard this unwrapping method as a kind of averaging procedure, in a similar way to noise reduction by speckle averaging in speckle interferometry.[11] It is important to realize, however, that whereas normally one averages over s *independent* random variables to obtain an improvement in signal-to-noise ratio of $\sqrt{s}$, in this case the $\Delta\Phi(t)$ values being averaged in Eq. (10) are clearly not independent. For example, $\Delta\Phi(t) = \Phi(t) - \Phi(t - 1)$ and $\Delta\Phi(t + 1) = \Phi(t + 1) - \Phi(t)$ so that $\Delta\Phi(t) + \Delta\Phi(t + 1) = \Phi(t + 1) - \Phi(t - 1)$ and errors in measuring $\Phi(t)$ automatically cancel out. In the same way, the only phase values contributing to errors in the final surface profile are those in the $t = 0$ and $t = s$ phase maps. One would therefore expect the error in surface height at a given point to vary as $1/s$ instead of $1/\sqrt{s}$. This result was checked by calculating the standard deviation in measured height for a small flat region (25 by 25 pixels) of the test plate from Fig. 2(a). The standard deviation is plotted in Fig. 5 versus the total phase range over the object {i.e., the variation in phase $[\Phi(s) - \Phi(0)]$ in going from the minimum to the maximum value of $(y \sin\alpha + z \cos\alpha)$}. As expected, the errors drop off as $1/s$ (solid curve) rather than as $1/\sqrt{s}$ (dashed curve). This has important implications for high-precision measurements because the time required to achieve a height accuracy of σ is proportional to σ and not to σ^2. The standard deviation at $s = 22$ images is 21.1 μm, which is 0.28% of the full depth range of the object. The groove depths obtained by averaging the data points within each groove from the cross section in Fig. 4(c) were 1.13, 2.15, and 4.12 mm, respectively.

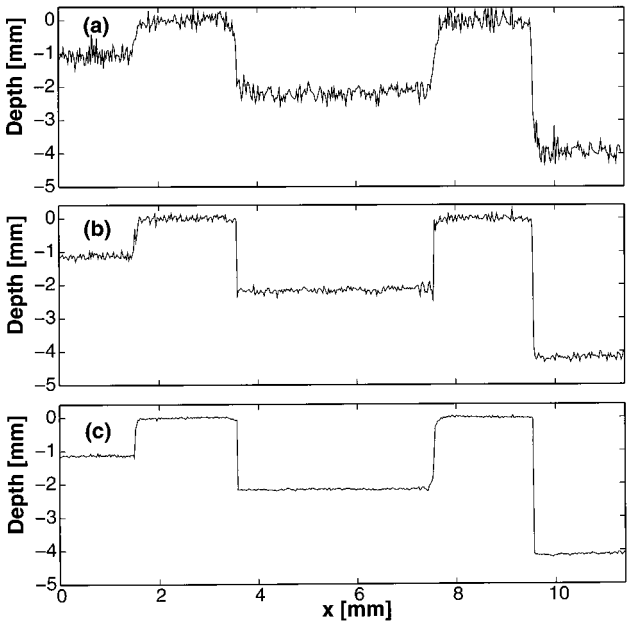

Fig. 4. Cross sections of a test object surface profile (central row of Fig. 3) obtained by unwrapping through (a) 1, (b) 6, (c) 22 incremental maps.

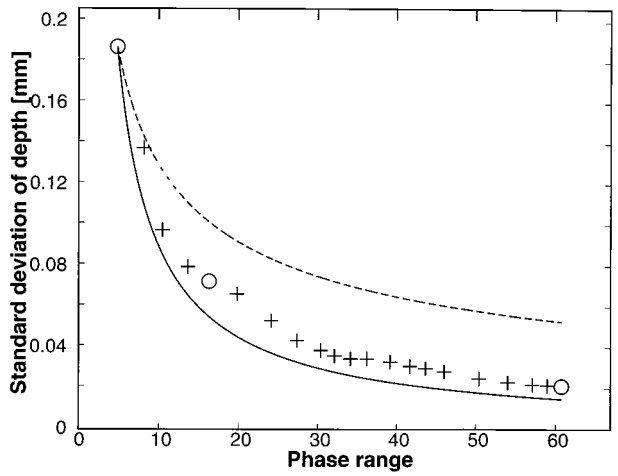

Fig. 5. Standard deviation in surface height as a function of the total phase range across the image. The circles correspond to the results shown in Fig. 4.

These compare well with the values 1.11, 2.09, and 4.08 mm measured at the same cross section on the sample with a conventional contacting dial gauge.

The decrease in error with increasing values of s can be expected eventually to level off as a result of other factors, one of the most important being a decrease in fringe visibility at high fringe density, which is due to the limited depth of field. The point at which this becomes an issue will clearly depend on the camera magnification and aperture ratio. Systematic errors that are due to miscalibration of the PZT phase shifter may also eventually become significant, and these would be expected to show up as a surface ripple with twice the spatial frequency of the sth fringe pattern.[7] This error source can be minimized by calibration of the PZT and by the use of calibration-insensitive phase-shifting algorithms.[7] However, neither of these factors limited the accuracy for the experiments described here.

Figures 6 and 7 show the result of unwrapping the phase maps of Fig. 2(b) (integrated circuit) and 2(c) (teeth) ($s = 22$ and 10, respectively). In the case of

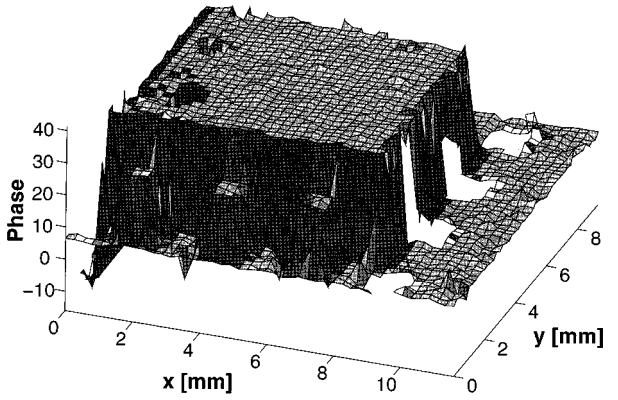

Fig. 6. Phase map of the integrated circuit from Fig. 2(b) unwrapped by the temporal phase-unwrapping algorithm, using 22 incremental maps.

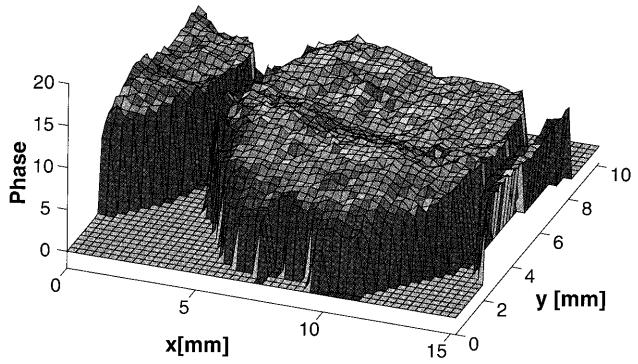

Fig. 7. Phase map of molar teeth from Fig. 2(c) unwrapped by the temporal phase-unwrapping algorithm, using ten incremental maps.

Fig. 6, two of the $\Delta\Phi(t)$ maps were found to have a phase range of more than $\pm\pi$ because there was too large a tilt of mirror M_1, and they were therefore dropped from the summation of Eq. (10). This situation would not arise if M_1 were controlled more precisely, for example by using a PZT. The noise levels are somewhat higher than for the test plate because of the much wider ranges of surface reflectivity: measurements on the integrated circuit, for example, had to cope with both the matte black plastic case and the highly reflective metal pins. Nevertheless, the heights of the case and pins relative to the Veroboard reference surface have been correctly determined. In the case of Fig. 7, the relative heights of the central molar and its two neighbors have also been correctly measured despite the lack of a continuous unwrapping path between them.

A working instrument based on the principle shown here would require automated tilting of the mirror, for example by means of a PZT. If a device with an integral displacement sensor is not available, then it must obviously be calibrated; however, because the intermediate phase values cancel out in the calculation of height, the usual nonlinear, hysteretic PZT response is not expected to be a significant problem. The only requirement for the PZT is that the total tilt angle between the first and last fringe patterns be consistent.

5. Conclusions

The combination of interferometrically generated projected fringes, phase stepping, and temporal phase unwrapping has resulted in a new and more powerful method of measuring surface profile. Unwrapping the measured phase at each pixel over time as the fringe pitch is changed allows measurement of absolute height at each pixel without reference to any of the neighboring pixels. In addition, aberrations in the optical system are canceled so that the only instrument calibrations required are those of the mirror-tilting and phase-stepping mechanisms. The first point means that profiles of objects containing height discontinuities can be measured as easily as smooth ones. Shad-

owing affects the images to the same extent as with conventional projected fringes, although phase errors are constrained to remain within the shadowed regions and not to propagate to affect regions of good signal-to-noise ratio, as is the case with conventional spatial unwrapping methods. Although many intermediate phase maps are required, the approach is inherently simple and robust. The height error at a given pixel varies inversely with the number s of phase maps through which the unwrapping is carried out, and a standard deviation of 0.28% of the full depth range of the object was obtained for $s = 22$. In principle this method could be implemented on a pipeline processor: a system using four phase steps per image, operating at 30 Hz, would unwrap through 20 images in under 3 s.

We are pleased to thank N.-E. Molin and L. R. Benckert for support and helpful discussions during the time the research was carried out. Useful comments from M. Sjödahl are also gratefully acknowledged.

References

1. R. E. Brooks and L. O. Heflinger, "Moiré gauging using optical interference patterns," Appl. Opt. **8,** 935–939 (1969).
2. G. Indebetouw, "Profile measurement using projection of running fringes," Appl. Opt. **17,** 2930–2933 (1978).
3. V. Srinivasan, H. C. Liu, and M. Halioua, "Automated phase-measuring profilometry of 3-D diffuse objects," Appl. Opt. **23,** 3105–3108 (1984).
4. D. R. Burton, A. J. Goodall, J. T. Atkinson, and M. J. Lalor, "The use of carrier frequency shifting for the elimination of phase discontinuities in Fourier transform profilometry," Opt. Lasers Eng. **23,** 245–257 (1995).
5. H. Zhao, W. Chen, and Y. Tan, "Phase-unwrapping algorithm for the measurement of three-dimensional object shapes," Appl. Opt. **33,** 4497–4500 (1994).
6. G. T. Reid, R. C. Rixon, and H. Stewart, "Moiré topography with large contour intervals," in *International Conference on Photomechanics and Speckle Metrology*, F.-P. Chiang, ed., Proc. SPIE **814,** 307–313 (1987).
7. K. Creath, "Temporal phase measurement methods," in *Interferogram Analysis*, D. W. Robinson and G. T. Reid, eds. (Institute of Physics, Bristol, 1993), pp. 94–140.
8. P. J. Caber, "Interferometric profiler for rough surfaces," Appl. Opt. **32,** 3438–3441 (1993).
9. J. M. Huntley and H. O. Saldner, "Temporal phase-unwrapping algorithm for automated interferogram analysis," Appl. Opt. **32,** 3047–3052 (1993).
10. K. A. Stetson, "Theory and applications of electronic holography," in *Proceedings of the International Conference on Hologram Interferometry and Speckle Metrology*, K. A. Stetson and R. J. Pryputniewicz, eds. (Society for Experimental Mechanics, Bethel, Conn., 1990), pp. 294–300.
11. K. Creath, "Averaging double-exposure speckle interferograms," Opt. Lett. **10,** 582–584 (1985).